This paper was presented as opening lecture at the Fourteenth Meeting "New Trends in Fatigue and Fracture" (NT2F14) Belgrade, Serbia, 15–18 September, 2014

Guy Pluvinage[1], Julien Capelle[1], Mohamed Hadj Méliani[2]

A REVIEW OF THE INFLUENCE OF CONSTRAINT ON FRACTURE TOUGHNESS

PREGLED UTICAJA GRANIČNIH USLOVA NA ŽILAVOST LOMA

Pregledni rad / Review paper
UDK /UDC: 539.42:539.551
Rad primljen / Paper received: 07.09.2014.

Adresa autora / Author's address:
[1)] LaBPS, Ecole Nationale d'Ingenieurs de Metz, France, pluvinage@cegetel.net
[2)] LPTPM, FS, Hassiba Ben Bouali University of Chlef, Algeria

Keywords
- constraint
- relative stress gradient
- T stress
- Q parameter

Ključne reči
- granični uslovi
- relativni gradijent napona
- T napon
- Q parametar

Abstract

Only constraint and stress gradient approaches to transferability of fracture toughness are examined.

Different constraint parameters are defined and discussed, and one example is given in each case. Factors that influence the constraint are studied. Special attention is given to the actual trends to use the plastic constraint in the Material Failure Master Curve (MFMC) and the Material Transition Temperature Master Curve (MTTMC). The paper also deals with the influence of T stress on the crack path and out-of-plane constraint and on the influence of thickness on fracture toughness.

Uses of plasticity with gradient and the relative stress gradient in local fracture approaches are also examined.

Izvod

Istraživanja u ovom radu obuhvataju granične uslove i gradijente napona u pristupu preslikavanja žilavosti loma.

Definisani su različiti parametri graničnih uslova sa diskusijom, i dat je po jedan primer za svaki slučaj. Proučeni su faktori koji utiču na granične uslove. Posebna pažnja je posvećena aktuelnim trendovima u primeni plastičnih veza kod master krive loma materijala (MFMC) i master krive prelazne temperature materijala (MTTMC). U radu je takođe obrađen uticaj T napona na putanju prsline i na granične uslove izvan ravni, kao i uticaj debljine na žilavost loma.

Takođe je proučena upotreba plastičnosti sa gradijentom i relativni gradijent napona u lokalnom pristupu loma.

INTRODUCTION

Mechanical properties are not intrinsic to material but depend on geometrical factors such as specimen geometry, thickness, surface roughness and length, defect geometry such as the relative length, radius, or opening angle, loading mode, and environment. Sinclair and Chambers /1/ have carried out fracture tests on brittle materials in plane strain conditions and on ductile materials in plane stress conditions and have found that classical linear fracture mechanics cannot predict fracture stress and is over-conservative.

If we consider two specimens that are geometrically identical but with different size, where the smallest is the model "*m*" and the second is the prototype "*p*", the ratio of geometrical dimensions including the crack length is equal to the scale factor λ.

For brittle material, if we assume that fracture toughness is intrinsic to material, the ratio of critical gross stress $\sigma_{g,c}$ is given by the following scaling law:

$$\frac{\sigma^m_{g,c}}{\sigma^p_{g,c}} = \sqrt{\lambda} \tag{1}$$

For ductile material this ratio is given by (Fig. 1):

$$\frac{\sigma^m_{g,c}}{\sigma^p_{g,c}} = \lambda^{1/N+1} \tag{2}$$

where N is the strain hardening exponent of the Ramberg-Osgood strain-stress law.

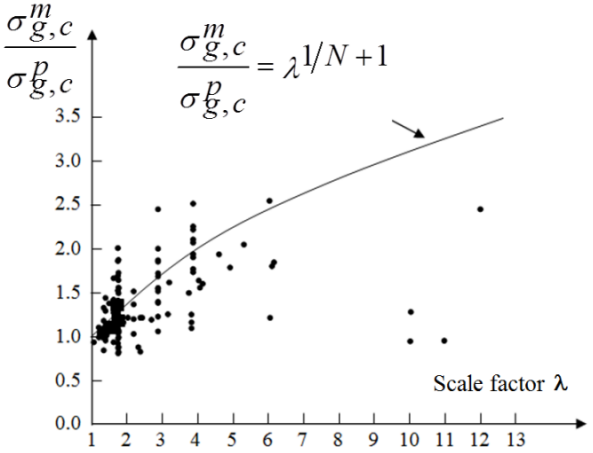

Figure 1. Scale effects on ductile fracture in plane stress. Experiments by Sinclair and Chambers /1/.
Slika 1. Uticaj razmere na duktilan lom pri ravnom stanju napona. Eksperimenti Sinklera i Čejmbersa /1/

Material properties available from databanks are therefore to be considered as reference material properties, as results from standard tests. To use these reference properties for a structure and component which differ in terms of geometry and loading mode, a correction needs to be made, which is called transferability.

The properties to be used in a structure P_{struct} are deduced from reference properties P_{ref} and the transferability function $f(p)$, where p is the transferability parameter.

$$P_{struct} = P_{ref}\, f(p) \tag{3}$$

Evidence of the scale effect was first pointed out by Leonardo da Vinci (1452-1519), and in the sixteenth century Galileo Galilei said that "from the small to the big is not so simple".

The scale effect is generally represented by models using a characteristic dimension from the structures. For probabilistic approaches /2/, the volume V of the structure, the scale factor λ /3/, or a characteristic length /3/ is used as an adjustable parameter.

A fractal approach to the scale effect on fracture toughness G_c was proposed by Carpinteri et al. /4/. It introduces a characteristic length l_{ch} which controls the transition from fractal to Euclidian behaviour.

Bazant /5/ has developed a scaling law based on an asymptotic and energetic approach. It refers to the critical stress, whose value is ruled by two asymptotic behaviours: plastic collapse without any scale effect, and brittle fracture where the scale effect is maximal. These two asymptotes intersect at a length D_0, which characterizes the brittle-to-ductile transition.

For fractures emanating from a defect where fracture mechanics can be applied, the transferability is sometimes treated with the concept of characteristic length or scale factor /6/ but more often by using the stress constraint or the relative stress gradient. These transferability parameters emanate from the defect tip distribution (notch or crack). If we compare the stress distribution obtained in a reference situation (generally small scale yielding) with another general one, the stress distribution is modified in two ways: there is a shift of the stress distribution and a small rotation. These modifications of the stress distribution are considered as transferability problems. The shift of the stress distribution is introduced into the plastic constraint, which is used as the transferability parameter. In literature, we can note the following constraint parameters: the plastic constraint factor L /7/, the stress triaxiality β /8/, the Q parameter /9/, T stress /10/, and A_2 /11/.

The rotation of the defect tip distribution is also less often used as a transferability parameter. The following parameters can be used: the strain gradient plasticity /12/, the defect tip relative stress gradient /13/, or the relative stress gradient /14/.

Today, there is no proposed approach combining these two aspects of the modification of the stress distribution with geometrical or loading mode parameters.

In this review paper, only constraint and stress gradient approaches to transferability are examined. For the characteristic length approaches, attention is focused instead on the scale effects /15/.

Different constraint parameters are defined and discussed and one example is given in each case. Factors that influence constraint are studied. Special attention is given to the plastic constraint in the Material Failure Master Curve (MFMC) and the Transition Temperature Master Curve (TTMC). The paper also deals with the influence of T stress on the crack path and the influence of thickness on fracture toughness with the out-of-plane constraint.

The use of plasticity with gradient and the relative stress gradient in local fracture approaches is also examined.

CONSTRAINTS AT DEFECT TIP

Constraint is considered as a modification of the defect tip distribution under the effects of specimen or defect geometries or loading mode. Different constraint parameters are defined and associated with the defect type or stress-strain behaviour.

Singular elastic stress distribution

For a notch with infinite acuity, Williams /16/ has given a solution for elastic stress distribution as the following series:

$$\sigma_{ij} = \sum_{n=1}^{\infty} Re\left[A_n r^{\lambda_n - 1} f_{ij}(\lambda_n, \theta)\right] \quad i,j = r,\theta \tag{4}$$

For a crack, Larson et al. /17/ have suggested describing the elastic stress field at the crack tip by three terms and introduce for the first time the T term as the second one of the series:

$$\sigma_{ij} = \frac{K_{ij}}{\sqrt{2\pi r}} f_{ij}(\theta) + \mathrm{T}\,\delta_{1i}\delta_{1j} + O\left(\sqrt{r}\right) \tag{5}$$

Therefore, ideally T stress is a constant stress which acts along the crack direction and shifts the opening stress distribution according to the sign of this stress (Fig. 2). For stress distribution emanating from a blunted crack or notch, T stress is not constant along the ligament. This leads to consider a conventional value defined as the effective T stress.

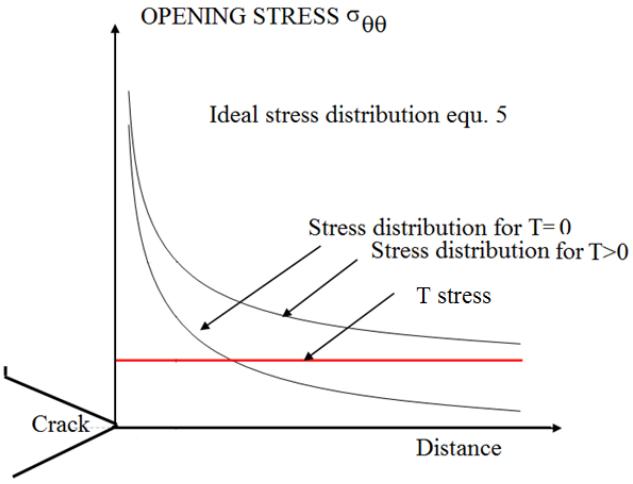

Figure 2. Ideal T stress distribution and shift of opening stress distribution by T stress.
Slika 2. Raspodela idealnog T napona i pomeranje raspodele napona otvaranja usled T napona

Singular elastic-plastic stress distribution

The power-law expansion of the elastic-plastic HRR /18/ field if higher-order singular or non-singular terms are considered, is represented by:

$$\sigma_{ij}(r,\theta)=\hat{A}_1\left[\left(\frac{r}{l}\right)^{s_1} f_{ij}^{(1)}(\theta)+\hat{A}_2\left(\frac{r}{l}\right)^{s_2} f_{ij}^{(2)}(\theta)+ \right. \\ \left. =\hat{A}_2^2\left(\frac{r}{l}\right)^{2s_2-s_1} f_{ij}^{(3)}(\theta)\right]+\ldots \quad (6)$$

with $s_1 = -1/(N + 1)$ and $\hat{A}_1 \sim J^{1/(N+1)}$, where N is the hardening exponent according to the Ramberg-Osgood constitutive equation, s_2 is the exponent of the second singular or non-singular term, J is a path integral, and l is a reference length.

O'Dowd and Shih /19, 20/ have simplified this formula. Considering strain hardening exponent values in the range $5 \le N \le 20$, the angular functions $f_{\theta\theta}$ and f_{rr} are equivalent and constant $f_{\theta\theta} \approx f_{rr} \approx$ constant, and the value of $f_{r\theta}$ is negligible when compared with $f_{\theta\theta}$ ($f_{\theta\theta} >> f_{r\theta}$) for $|\theta| < \pi/2$. The stress field is therefore described by:

$$\sigma_{ij}=\left(\frac{J}{B_0 I_n r}\right)^{\frac{1}{n+1}} f_{ij}(\theta,n)+Q\left[\frac{r}{J/\sigma_0}\right]^{q} f_{ij}(\theta,n)+\ldots \quad (7)$$

B_0 and I_n are constants for fixed values of θ and n; q is a parameter close to zero ($q \approx 0$); and σ_0 is the reference stress. The Q parameter is called the amplitude factor of the second-order field or simply Q.

Non-singular elastic and elastic plastic stress distribution

The opening stress at the notch tip exhibits a more complex distribution. The stress increases until it reaches a maximum, which occurs behind the notch tip at distance x_{max}. At distance X_{ef} (the effective distance), the distribution is governed by a power law with an exponent close to those given by the elastic stress distribution of Williams /16/. In Fig. 3, zone III represents precisely this zone, where the stress distribution exhibits a linear behaviour in the bi-logarithmic diagram and is governed by the notch stress intensity factor. In zone IV, the stress distribution decreases until it reaches the gross stress level. The effective distance X_{ef} corresponds to the minimum of the relative stress gradient.

THE DIFFERENT CONSTRAINT PARAMETERS

To assess the effect of geometry and loading mode on fracture toughness, different two-parameter concepts are applied as K–T stress- and J–A2-concepts based on a rigorous description of the asymptotic fields as well as the phenomenological J–Q- and J–β-concepts using the Q-parameter and the stress triaxiality β as secondary fracture parameters.

T stress

The stress distribution ahead of a crack tip depends on the polar angle θ, as we can see in Eq.(2). However for some particular θ angles, the T stress is given by particular values of the difference between the opening stress σ_{yy} and the stress parallel to the crack σ_{xx} (see Table 1).

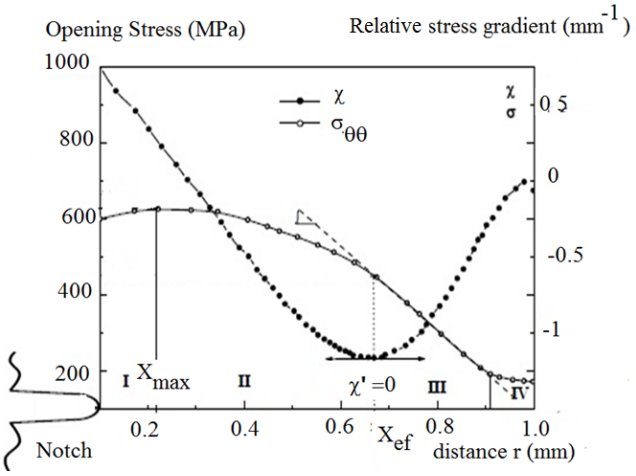

Figure 3. Elastic-plastic stress distribution and definition of effective distance from the minimum of the relative stress gradient.
Slika 3. Raspodela elastoplastičnih napona i definicija efektivnog rastojanja od minimuma relativnog gradijenta napona

Table 1. T stress values according to polar direction θ.
Tabela 1. Vrednosti T napona sa polarnim pravcem θ

$\theta = 0$	$\theta = \pm\pi$	$\theta = \pm\pi/3$	$\theta = \pm\pi/2$	$\theta = \pm 2\pi/3$
$T = (\sigma_{xx} - \sigma_{yy})$	$T = \sigma_{xx}$	$T = \sigma_{xx} - \sigma_{yy}/3$	$T = \sigma_{xx} - \sigma_{yy}/3$	$T = (\sigma_{xx} - \sigma_{yy})$

Particularly for $\theta = 0$, the T stress is given by:

$$T = (\sigma_{xx} - \sigma_{yy})_{\theta=0} \quad (8)$$

Equation (8) is the basis of the so-called stress difference method, which was proposed by Yang et al. /21/. The stress distribution in the direction $\theta = 0$ is generally computed by the finite element method. Chao et al. /22/ computed σ_{xx} in the direction $\theta = 180°$ (in the crack back direction) by the finite element method and defined the T stress as the value of σ_{xx} in the region where the value is constant. Ayatollahi et al. /23/ determined the T stress by using the Displacement Method in the finite element and then obtained a stabilized T stress distribution along the ligament.

T-stress can be measured experimentally using strain with the difference between the normal strains in polar coordinates after a rotation of the angle α /24/. From Williams's solution, the strain difference is given by:

$$E(\varepsilon_{rr}-\varepsilon_{\theta\theta}) = A_1 r^{-0.5}(1+\nu)\sin\theta\left[\cos\frac{3\theta}{2}\sin 2\alpha - \sin\frac{3\theta}{2}\cos 2\alpha\right]+ \\ +2A_2 r^{0}(1+\nu)\cos 2\alpha + \\ +A_3 r^{0.5}(1+\nu)\sin\theta\left[\sin\frac{\theta}{2}\cos 2\alpha - \cos\frac{\theta}{2}\cos 2\alpha\right]+ \\ +2A_4 r^{1}(1+\nu)\left[\cos\theta + \cos 2\alpha - 2\sin\theta\sin 2\alpha\right] \quad (9)$$

Here, E and ν are the Young's modulus and Poisson's ratio, respectively, the value of A_1 is proportional to the stress intensity factor K_I, and the parameter A_2 is proportional to the T-stress. For the angles $\theta = \pm 120°$ (MM line of Fig. 4), Eq.(9) can be simplified and leads to the following approximation for small values of r:

$$\frac{E}{(1+\nu)}(\varepsilon_{xx}-\varepsilon_{yy}) \sim 2A_2 \quad (10)$$

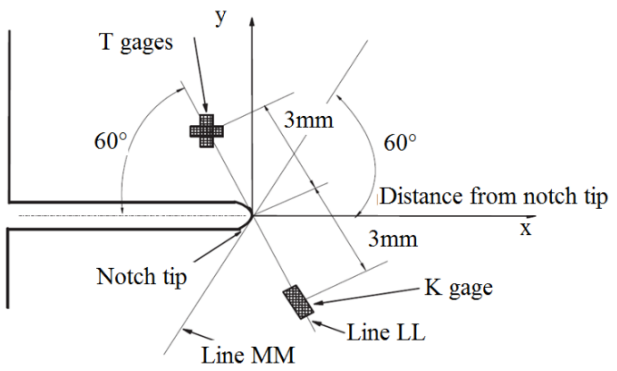

Figure 4. Experimental determination of T stress using strain gauges, here $\alpha = 60°$ /24/.
Slika 4. Eksperimentalno određivanje T napona korišćenjem mernih traka, ovde je $\alpha = 60°$ /24/

Physically, T stress is acting parallel to the crack line in x direction with amplitude proportional to the gross stress. T may be positive (tensile) or negative (compression).

An example of the computed T stress distribution along the ligament for a Roman tile specimen with a notch is given in Fig. 5. It can be seen that T is not really constant as it is in theory. For short cracks, distribution of the T stress is stabilized after some distance. For long cracks, T increases linearly with the ligament except in a region close to the crack tip. To avoid this dependence of the T stress on distance, it is attractive to use a conventional definition of the effective T stress.

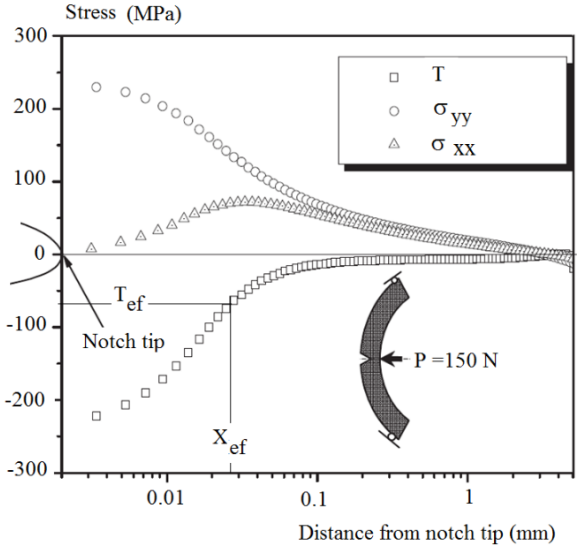

Figure 5. T stress evolution with distance for a Roman tile specimen. Values of T_{ef} parameter obtained by extrapolation or volumetric methods.
Slika 5. Razvoj T napona sa rastojanjem kod epruvete „rimski crep“. Vrednosti parametra T_{ef} dobijeni su ekstrapolacijom ili volumetrijskom metodom

Maleski et al. /25/ suggested representing the T stress evolution by a linear relationship with distance x:

$$T(x) = T_{ef} + \gamma^{*}(x/a) \tag{11}$$

where γ^{*} is a constant and a is the crack depth. T_{ef} is obtained by extrapolation $x \to 0$. Using the volumetric method, Hadj Meliani et al. /10/ suggested defining the effective T stress as the corresponding value in the T stress distribution for a distance equal to the effective distance X_{ef}. Figure 5 gives the T stress evolution with distance for a Roman tile specimen and the definition of T_{ef}. One notes that in this case the values of T_{ef} obtained by extrapolation or the volumetric method are relatively close. In the following, the T_{ef} parameter obtained from the critical stress distribution is called $T_{ef,c}$.

Q Parameter

In Eq.(5) the J-integral sets the size scale over which high stresses develop while the second parameter, Q, quantifies the level of some stress shift at distances of a few CTODS ahead of the crack tip; such a dimension defines the physically relevant length scale of the fracture process zone X_{ef}.

The constraint has been defined by Dodds et al. /26/ using the Q parameter. This parameter is defined as the difference between the opening stress level for a given geometry or loading mode and a reference situation with generally small scale yielding (ssy) divided by the reference stress σ_0.

$$Q = \frac{\sigma_{\theta\theta} - (\sigma_{\theta\theta})_{ssy}}{\sigma_0} \tag{12}$$

O'Dowd and Shih /19, 20/ showed that Q corresponds effectively to a spatially uniform hydrostatic stress and represents the relative difference between the high triaxiality reference stress field and that of the fracture specimen. Q is defined at a non-dimensional distance of $\sigma_0 \cdot r/J = 2$. In order to fulfil the condition of a spatially uniform Q, it is necessary that the reference and the studied stress field be homothetic, /26/. The following conditions are added for a correct determination of Q:

$$\text{grad}Q = \frac{Q_{(1)} - Q_{(5)}}{4} \le 0.1 \tag{13}$$

where $Q_{(1)}$ and $Q_{(5)}$ are Q values determined respectively at the non-dimensional distances 1 and 5 (Fig. 6).

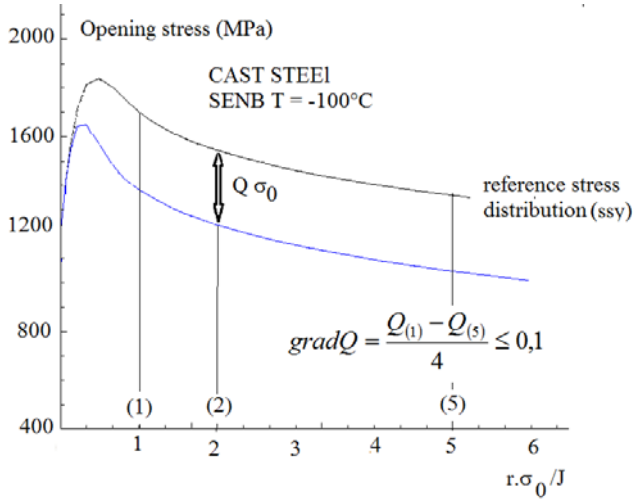

Figure 6. Definition of Q parameter and validity condition.
Slika 6. Definicija parametra Q i uslov važenja

If the condition given by Eq.(13) is satisfied, the stress distributions corresponding to the small scale yielding and the studied one are homothetic. Here, we considered a local

fracture criterion for brittle fracture with two parameters, the critical stress σ_c and the characteristic distance X_c. The characteristic distance is in this case independent of the stress distribution and is associated with a material characteristic if we multiply the relationship (12) by $\sqrt{\pi X_c}$:

$$Q = \frac{\sigma_{yy}\sqrt{\pi X_c} - (\sigma_{yy})_{SSY}\sqrt{\pi X_c}}{\sigma_y \sqrt{\pi X_c}} \tag{14}$$

and multiply again by the geometry correction factor F:

$$Q = \frac{K_c - K_{Ic}}{\sigma_y \sqrt{\pi X_c} F} \tag{15}$$

we can see that in this case Q is simply the relative difference between critical stress intensity factors.

Stress triaxiality

The stress triaxiality β is also used as a measure of the constraint and leads to the two-parameter fracture mechanics approach K–β or J–β. Stress triaxiality is chosen as a transferability parameter because ductile fracture is sensitive to this parameter through void growth /27/ as well as cleavage stress for brittle fracture /28/.

This parameter is defined as the ratio of the hydrostatic stress over the equivalent von Mises stress.

$$\beta = \frac{\sigma_h}{\sigma_{VM}} \tag{16}$$

where
$$\beta\sigma_h = \frac{\sigma_{xx} + \sigma_{yy} + \sigma_{zz}}{3} \tag{17}$$

and
$$\sigma_{VM} = \frac{1}{\sqrt{2}}\sqrt{(\sigma_1 - \sigma_3)^2 + (\sigma_1 - \sigma_2)^2 + (\sigma_2 - \sigma_3)^2} \tag{18}$$

The critical stress triaxiality distribution at the notch tip increases until it reaches a maximum, which for the critical event is called $\beta_{\max,c}$ and corresponds to distance $X_{\beta\max,c}$. After that, it decreases, then sometimes increases again, and finally falls to zero when the distance is far from the notch tip.

The maximum critical stress triaxiality is sensitive to the notch radius and ligament size. It decreases practically linearly with the notch radius and increases with relative notch depth /29/. It has been noted that the maximum triaxiality always occurs inside the fracture process zone since $X_{\beta\max,c}$ remains lower than or equal to the critical effective distance $X_{ef,c}$ /29/.

With an increase of the relative notch depth, the position of maximum stress triaxiality approaches or reaches the limit of the fracture process zone.

According to /29/, the maximum stress triaxiality parameter is not the most suitable constraint parameter to explain the modification of fracture toughness with ligament size or thickness. An improvement has been made using the effective critical stress triaxiality $\beta_{ef,c}$. This parameter is defined as the average value of the critical stress triaxiality over the critical effective distance $X_{ef,c}$.

$$\beta_{ef,c} = \frac{1}{X_{ef,c}} \int_0^{X_{ef,c}} \beta(x)dx \tag{19}$$

Other constraint parameters

A_2 and A_3 parameters

A three-term asymptotic solution for stresses near the tip of the crack in an elastic-plastic body can be written in the form /11/:

$$\frac{\sigma_{ij}}{\sigma_0} = \tilde{A}_1 \bar{r}^s f_{ij}^0 + \tilde{A}_2 \bar{r}^t f_{ij}^1 + \tilde{A}_3 \bar{r}^{2t-s} f_{ij}^2 \tag{20}$$

where $\bar{r}$ is the dimensionless distance:

$$\bar{r} = \sigma_0 \frac{r}{J} \tag{21}$$

t and s are exponents, and σ_0 is the reference stress. f_{ij}^0, f_{ij}^1, and f_{ij}^2 are normalized angular functions obtained from the solutions of asymptotic problems. A_1 and A_2 are two independent amplitudes found by stress fitting inside the fracture process volume.

$$\tilde{A}_1 = \left(\frac{J}{\alpha\varepsilon_0\sigma_0 I_n l}\right)^{-s} \quad s = -\frac{1}{n+1} \tag{22}$$

The dimensionless integration constant I_n depends only on the hardening exponent n and is independent of other material constants (i.e. reference strain ε_0 or stress σ_0, respectively) and applied loads. L is a characteristic length parameter which can be chosen as the crack length a, the specimen width W, the thickness B, or unity. α is a parameter of the Ramberg-Osgood law.

A_3 depends on A_1 and A_2:

$$\tilde{A}_3 = \frac{\tilde{A}_1^2}{\tilde{A}_2} \tag{23}$$

$\tilde{A}_1$ is related to J, and $\tilde{A}_2$ is related and close to Q. The constraint parameter $\tilde{A}_2$ is determined as presented by Nikishkov, /11/, by comparison of the actual radial and circumferential stresses distribution in the specimen and the stresses according to the reference asymptotic field at two points located in the ligament and at $\theta = \pi/4$, both at a distance of $r = 2J/\sigma_0$. This procedure is identical to those used for Q determination.

$\tilde{A}_3$ can be used for a three-parameter fracture approach, K–T–A_3 or J–A_2–A_3 /22, 30-31/.

Plastic constraint factor

The plastic constraint factor is used for determination of the limit state. The theory of limit analysis appeared in the late 1930s. It constitutes a branch of the theory of plasticity related to an elastic perfectly plastic behaviour. In the mid-1950s a large number of analytical solutions appeared for calculating the ultimate load of beams and shells, leading to more realistic values of the capacity to resist plastic collapse.

The introduction of linear fracture mechanics in the mid-1950s led to consider the risk of brittle fracture governed by the global stress in apparent opposition to the theory of plastic collapse governed by the net stress.

This failure criterion assumes that failure occurs when a critical net stress σ_N^c reaches the ultimate strength R_m. One notes that ductile failure is sensitive to net stress σ_N (load divided by the ligament cross-section) while brittle fracture

is sensitive to gross stress σ_g (load divided by the entire section). The above-mentioned criterion needs to be modified to take into account constraints due to geometry and loading mode effects in the following manner:

$$\sigma_N^c = L \cdot R_m \tag{24}$$

where L is the so-called plastic constraint factor.

Design codes are based on limit analysis to calculate the limit state and incorporate the safety factor through the lower bound of a plot of experimental results.

Figure 7 gives the evolution of the plastic constraint factor in a polyethylene pipe with a semi-elliptical surface defect. The plastic constraint factor L is plotted versus the relative defect depth a/D, where D is the pipe diameter.

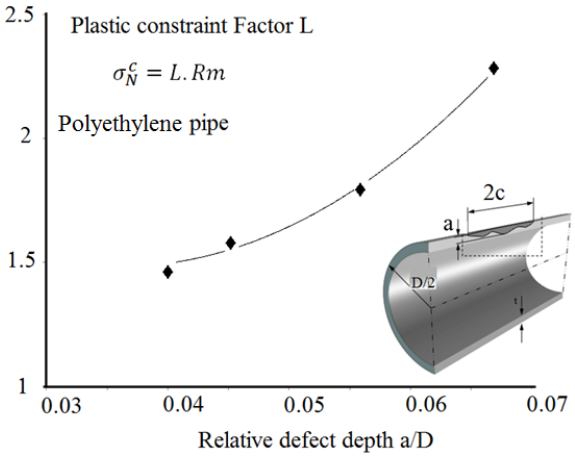

Figure 7. Evolution of the plastic constraint factor versus the relative defect depth a/D. Polyethylene pipe, /7/.
Slika 7. Razvoj faktora plastičnog graničnog uslova prema relativnoj dubini greške a/D. Polietilenska cev, /7/

Constraint parameter φ or A_p

T stress has a strong influence on the shape and size of the plastic zone /30/. For example, in plane strain the plastic zone has a typical shape of a butterfly wing. For a positive T stress the wings are oriented in the crack as above direction. If the T stress is negative, the wings are oriented in the reverse crack extension direction, /31/.

This effect is illustrated in Fig. 8, showing the plastic zone ahead of a surface notch defect. This defect is located in a pipe of diameter D and thickness B (B = 8.9 cm). The applied internal pressure is 20 bar.

The size of the plastic zone is also modified because the equivalent stress is modified by the T stress. If we consider the asymptotic field given by Eq.(3) and $\theta = \pi$, the equivalent von Mises stress σ_{eq} is a function of the ratio T/K_I:

$$\sigma_{eq}(r,\theta=0,\ \nu=1/3) = \frac{1}{3}\frac{K_I}{\sqrt{2\pi r}}\sqrt{\frac{27}{28}+\frac{1}{28}\left(1+\frac{14T\sqrt{2\pi r}}{K_I}\right)^2} \tag{25}$$

When T is negative (specimen in tension), the plastic zone increases compared to the reference case for which T = 0. For positive values of T (double cantilever beam, DCB, or compact tension, CT, specimen), the size of the plastic zone decreases.

Mostafavi et al., /32/ have suggested a new constraint parameter φ defined as the ratio of the current plastic zone area $A_{p,c}$ and the reference plastic zone area, that is, for a small scale yielding situation $A_{p,ssy}$.

$$\varphi = \frac{A_{p,c}}{A_{p,ssy}} \tag{26}$$

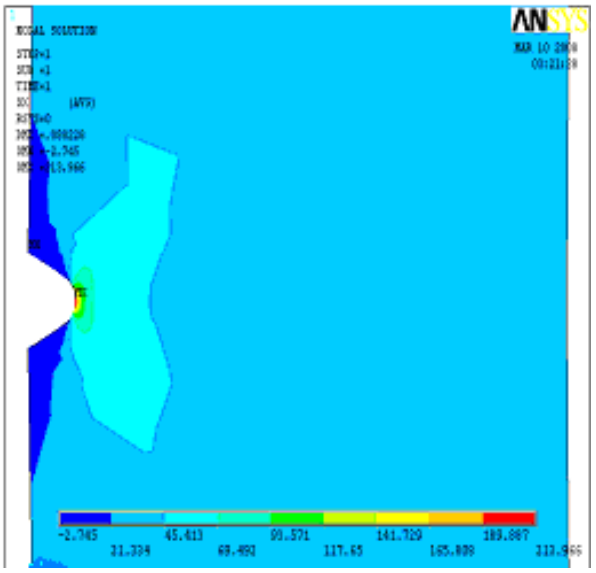

$a/t = 0.1$ $R/t = 20$ $T < 0$

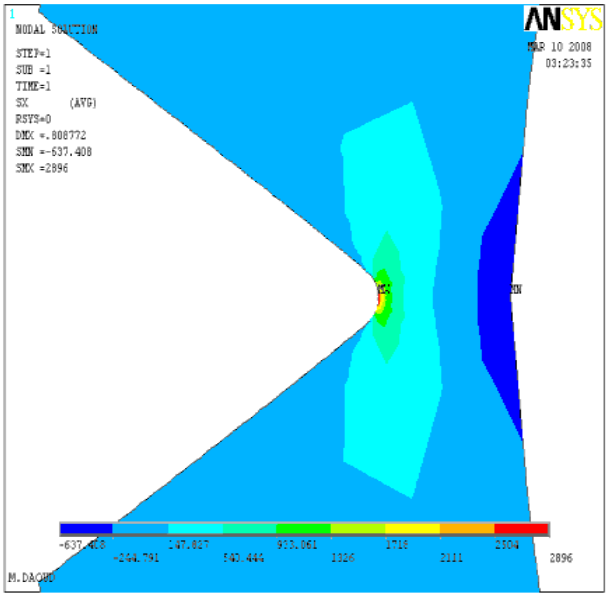

$a/t = 0.75$ $R/t = 20$ $T > 0$

Figure 8. Influence of T stress sign on plastic zone shape.
Slika 8. Uticaj predznaka T napona na oblik plastične zone

Mostafavi et al., /32/, remarked that the constraint parameter φ has its limitation in characterizing the constraint at a higher J-integral value for ductile material and suggested that the constraint definition be modified by a new parameter A_p:

$$A_p = \frac{A_{\varepsilon p,c}}{A_{\varepsilon p,ref}} \tag{27}$$

$A_{\varepsilon p,c}$ is the area surrounded by the equivalent plastic strain (ε_p) isolines ahead of the crack tip and $A_{\varepsilon p,ref}$ is the reference area surrounded by the (ε_p) isolines in a standard test.

Yang et al. /33/ found that a sole linear relation between the ratio of the current and the reference fracture toughness J_C/J_{ref} exists. This is restricted to the case for dissimilar metal welded joints regardless of the in-plane and out-of-plane constraints for a crack. This relationship is independent on the selection of the ε_p isolines for higher ε_p values and can be regarded as a unified reference line to characterize the dependence of fracture resistance of a crack on the constraint (Fig. 9).

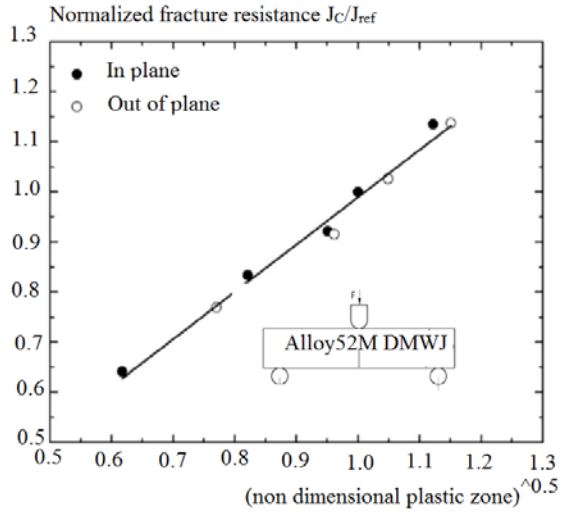

Figure 9. Normalized fracture resistance J_C/J_{ref} versus $\sqrt{A_p}$ for cracked dissimilar metal welded joints, obtained from $\varepsilon_p = 1.0$ isolines, /33/.

Slika 9. Normalizovana otpornost prema lomu J_C/J_{ref} sa $\sqrt{A_p}$ za naprsle zavarene spojeve raznorodnih metala, dobijeno iz $\varepsilon_p = 1{,}0$ izolinija, /33/

FACTORS OF INFLUENCE ON CONSTRAINT

Values of the constraints T_{ef}, Q, and stress triaxiality are sensitive to specimen geometry, loading mode, ligament size, and load level, /34/. Some examples of these effects are given as follows.

Loading mode

It has been noted that T stress can be negative or positive. In Table 2, the critical effective T stress for four specimens used for fracture test has been reported. These specimens have a notch of 0.25 mm radius and are made in X 52 pipe steel. Four types of specimens are examined: single edge notch tensile (SENT), CT, Roman tile (RT), and DCB.

Table 2. Values of $T_{ef,c}/\sigma_y$ for four specimen types (SENT, CT, RT, and DCB).

Tabela 2. Vrednosti $T_{ef,c}/\sigma_y$ za četiri tipa epruveta (SENT, CT, RT, i DCB)

Specimen	SENT	CT	RT	DCB
$T_{ef,c}/\sigma_y$	[–0.74; –0.80]	[–0.53; –0.67]	[–0.25; –0.30]	[+0.19; +0.21]

In general, specimens loaded in tension like CCT or SENT have a high negative effective T stress and are therefore less constrained. Specimens in bending like TPB or CT have lower negative T stress and higher constraint, /10/. DCB always has positive values. In the next section, we will discuss the consequence for crack bifurcation.

For the CT specimen, some contradictory results can be found in literature, /35/. The effective T stress is sometimes negative and sometimes positive. These differences can be explained by the definition of the effective T stress, the ligament size, the load level, and so on.

Thickness

The effect of thickness on constraint is explained later as the effect of out-of-plane constraint, /35/.

Ligament size

Figure 10 depicts the constraint parameter T_{ef} distribution for the CT specimen (width W = 63.80 mm, height = 61 mm, thickness = 5.84 mm, notch radius = 0.25 mm) in plane stress. The relative notch depth a/W varies in the range 0.1 to 0.7 and the applied load is constant for each value of a/W and equal to 1000 N. The value of effective T stress T_{ef} is associated with the effective distance, which varies with a/W, /10/.

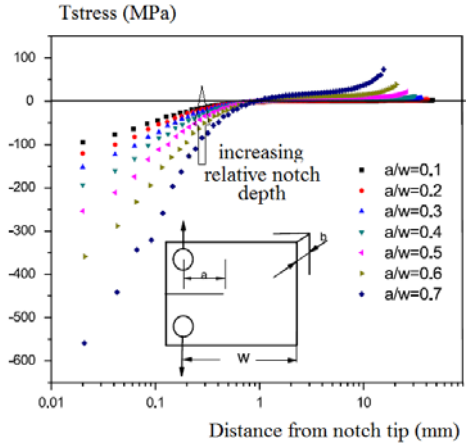

Figure 10. T_{ef} distribution for CT specimen (width W = 63.80 mm, height 61 mm, thickness 5.84 mm, notch radius 0.25 mm) in plane stress, /10/.

Slika 10. T_{ef} raspodela za CT epruvetu (širina W = 63,80 mm, visina 61 mm, debljina 5,84 mm, poluprečnik zareza 0,25 mm) pri ravnom stanju napona, /10/

One notes that the value of T_{ef} increases when a/W increases. This result is confirmed by /40/, where T, Q, β, and A_2 are computed for a clamped single-edge tension specimen. The relative crack depth varies in the range a/W = 0.3–0.7 at the loading level of $J/(b\sigma_0) = 0.01$, where b is the ligament size. These authors indicate that, in general, T, $-Q$, β, and $-A_2$ increase as a/W increases; however, the impact of a/W is relatively small.

Loading path in plane K_{ap}-T_{ef}

A negative value of the T_{ef}-parameter increases with the applied load generally according to a parabolic function for low values of the applied load or pressure and becomes practically linear when the load value increases. In the plane applied stress intensity factor-effective T stress, all the assessment points follow a non-linear curve, which is the so-called loading path. The loading path intercepts the MFMC at the point $K_{\rho,c}$–$T_{ef,c}$ -parameter (or K_c if the defect is a crack) at the critical event. Figure 11 gives an example of different loading paths for a pipe made of X52 steel. The

pipe exhibits a longitudinal surface notch defect with relative depth a/B: a/B = 0.1, 0.3, 0.5, and 0.75, and relative radius R/B = 40, where B is the wall thickness of the pipe.

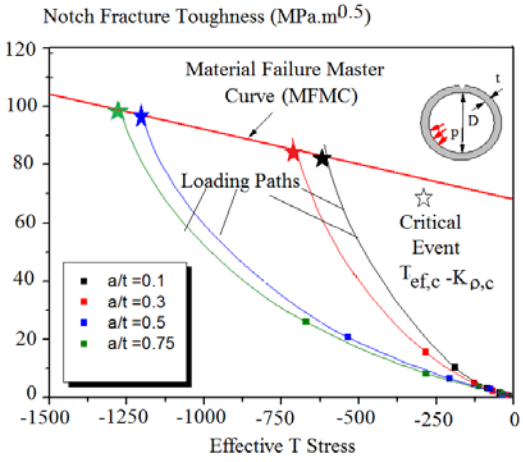

Figure 11. Loading path and Material Failure Master Curve (MFMC) for a pipe with a longitudinal surface notch defect: a/B = 0.1, 0.3, 0.5, and 0.75 and R/B = 40, /10/.
Slika 11. Krive opterećenja i master kriva otkaza materijala (MFMC) za cev sa podužnom površinskom greškom tipa zareza: a/B = 9,1; 0,3; 0,5 i 0,75, kao i R/B = 40, /10/

INFLUENCE OF CONSTRAINT ON FRACTURE TOUGHNESS

Eisele et al. /36/ pointed out that fracture toughness K_c or J_c increases with the loss of constraint T stress, A_2 or Q.

This can been seen in Fig. 12, where the J_C-Q locus of a low carbon manganese cast steel is plotted, /37/. Three-point bending tests were used for fracture behaviour determination. Fracture toughness was determined using three test specimen geometries. The first one was the standard three point bend specimen 25 × 50 × 220 mm with a ratio a/W = 0.5. The other ones were selected to receive shallow cracks (specimen 1: a/W = 0.1; 25 × 30 × 130 mm; specimen 2: a/W = 0.2; 25 × 27 × 120 mm). The stress distribution using the standard method for Q-parameter determination was computed by the finite element method at load level corresponding to the fracture force.

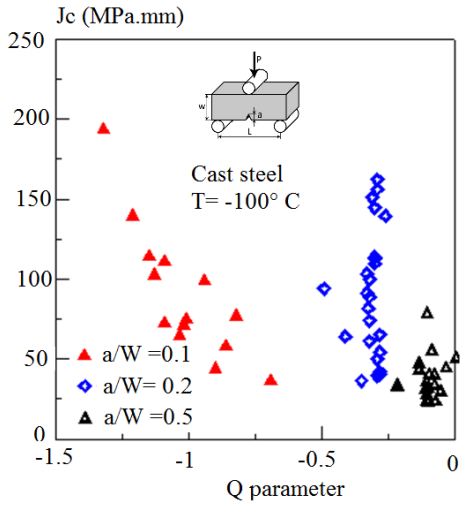

Figure 12. J_C-Q locus of a low carbon manganese cast steel /37/.
Slika 12. J_C–Q lokus za niskougljenični manganski čelični liv /37/

One notes that the fracture toughness decreases when the constraint increases; that is, the Q-parameter increases.

Hadj Meliani et al. /10/ have also pointed out this effect on the notch fracture toughness $K_{\rho,c}$ with the critical constraint described by the T_{ef}-parameter. The material used in this study is API X52 steel.

Several specimens of four types, namely CT, DCB, SENT, and RT, are extracted from a steel pipe of diameter 610 mm. The geometries of these specimens are as follows: SENT specimen: thickness = 5.8 mm, width = 58.40 mm; CT specimen: thickness = 5.8 mm, width = 63.80 mm, height = 61 mm; DCB specimen: thickness = 5.8 mm, height = 45.70 mm; RT specimen: thickness = 5.8 mm, width = 40 mm, length = 280 mm. The specimens have a notch with a notch angle ψ = 0 and a notch radius ρ = 0.25 mm and an a/W ratio in the range 0.3–0.6. The stress distribution used is computed by the finite element method at a load level corresponding to the fracture force. $T_{ef,c}$ is determined by the volumetric method. It can be noted in Fig. 13 that the fracture toughness decreases linearly with the constraint according to

$$K_{\rho,c} = aT_{ef,c} + K^0_{\rho,c} \tag{28}$$

where $K^0_{\rho,c}$ is the fracture toughness corresponding to $T_{ef,c}$ = 0, which is considered as a reference. a = −0.069 and $K^0_{\rho,c}$ = 77.2 MPa√m for the API X52 pipe steel.

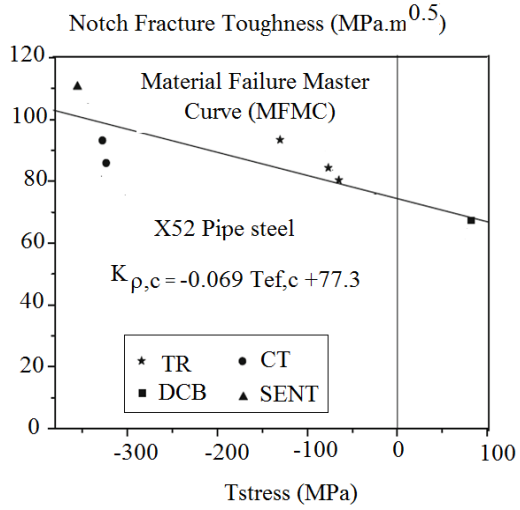

Figure 13. $K_{\rho,c}$–$T_{ef,c}$ locus of a low carbon manganese cast steel /10/.
Slika 13. $K_{\rho,c}$–$T_{ef,c}$ lokus za niskougljenični manganski čelični liv /10/

INFLUENCE OF CONSTRAINT ON TRANSITION TEMPERATURE

Wallin /38/ has established a new MFMC, where the fracture toughness K_c is a function of the temperature T and the T stress. The standard master curve K_0 corresponding to a reference temperature T_0 has the form

$$K_0 = 31 + 77\exp(0.019[T - T_0]) \tag{29}$$

T_0 is the transition temperature corresponding to a conventional value of fracture toughness of 100 MPa√m. Materials that have a similar exponential evolution of fracture toughness with temperature T are characterized by a single parameter T_0.

In order to account for the constraint effect in the MFMC, Wallin /38/ assumed that the reference temperature is constraint dependent. A linear relation is found between the reference temperature T_0 and the T stress.

$$T_0(T) = T_{0,ref} \quad \text{for} \quad T_{stress} > 0$$

$$T_0(T_{stress}) = T_{0,ref} + \frac{T_{stress}}{10} \frac{^\circ\text{C}}{\text{MPa}} \quad \text{for} \quad T_{stress} < 0 \qquad (30)$$

$T_{0,ref}$ is the reference temperature for a reference constraint as obtained for small scale yielding or for $T_{stress} = 0$.

More generally, Wallin /39/ proposed:

$$T_0 = T_{0,T=0} + \frac{A T_{stress}}{\sigma_y} \qquad (31)$$

where A is new parameter. To assess the validity of Eq. (31), Hohe et al. /40/ presented the results of fracture resistance of nuclear grade 22 NiMoCr 3–7 pressure vessel steel as a linear regression analysis of both the fracture toughness K_{Jc} and the respective secondary fracture parameter Y (T_{stress}/σ_0, Q, A_2, or β respectively).

$$T_0 = cY + d \qquad (32)$$

The parameters c and d are determined by means of a least squares minimization. The results are given in Table 3 and in Fig. 14 where the transition temperature T_0 is plotted versus T/σ_0 with σ_0 the reference stress. Table 3 shows the linear regression parameters for the constraint dependence of the reference temperature, reference constraint value, and constraint indexing master curve reference temperature T_0^{CI} /40/.

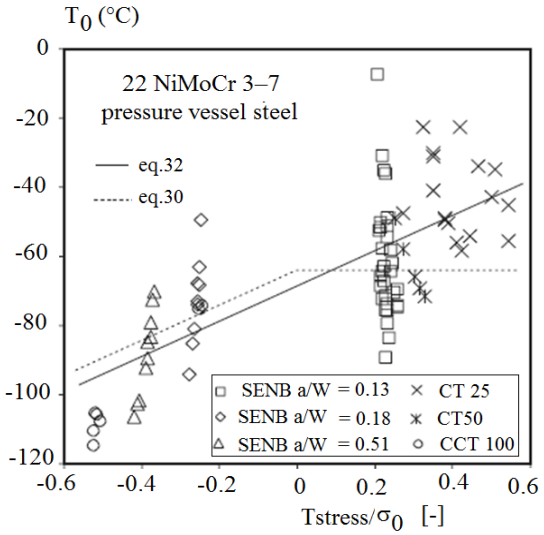

Figure 14. Linear regression analysis of both the fracture toughness K_{Jc} and the respective secondary fracture parameter Y (T_{stress}/σ_0, Q, A_2, or β respectively), /40/.
Slika 14. Linearna regresiona analiza žilavosti loma K_{Jc} i odgovarajućeg sekundarnog parametra Y (T_{stress}/σ_0, Q, A_2 ili β respektivno), /40/

A similar relation was found for X65 pipe steel by Coseru et al. /41/ between various transition temperatures T_t ($T_{t,tensile}$, T_0, and $T_{K1/2}$) and the critical effective T stress, $T_{ef,c}$.

$$T_t = T_{t,Tef.c=0} + 0.14 T_{ef,c} \qquad (33)$$

This equation represents the Material Transition Temperature Master Curve (MTTMC) $T_t = f(T_{ef,c})$, which is the key to determining the appropriate reference transition temperature by comparison with the structure transition temperature.

Table 3. Parameters of linear regression analysis using Eq.(32) for fracture resistance of nuclear grade 22 NiMoCr 3-7 pressure vessel steel.
Tabela 3. Parametri analize linearne regresije preko formule (32) za otpornost na lom čelika za posude pod pritiskom tipa 22 NiMoCr 3-7

Y	c (°C)	c (°C)	Y_{ref}	T_0^{CI} (°C)
T_{stress}/σ_0	51.4	–68.6	0.40	–56.9
Q	47.2	–59.8	0.20	–53.9
A_2	203.4	–0.16	–0.20	–55-8
β	40.6	–157.0	2.72	–53.7

In Figure 15, the determination of the MTTMC of API X65 pipe steel is done using three specimen types (tensile, CT, and Charpy) /41/. Different Charpy specimens are used: Charpy V specimens (V notch, notch radius $\rho = 0.25$ mm, notch depth $a = 2$ mm), Charpy U_1 (U notch, notch radius $\rho = 1$ mm, notch depth $a = 5$ mm), and Charpy $U_{0.5}$ (U notch, notch radius $\rho = 0.5$ mm, notch depth $a = 5$ mm), and the transition temperatures of Charpy specimens are corrected to take into account the influence of the loading rate.

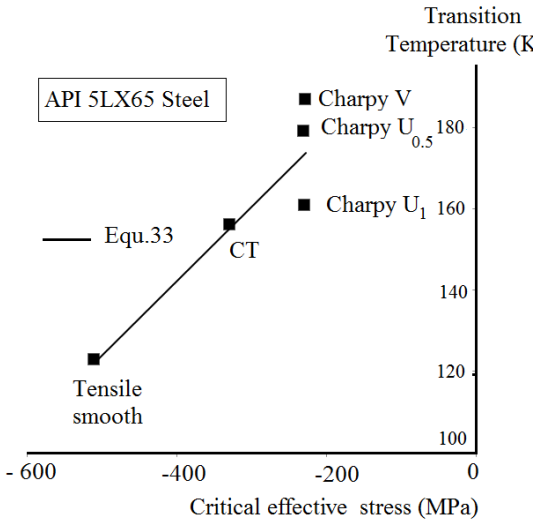

Figure 15. The MTTMC of API X65 pipe steel, /41/.
Slika 15. MTTMC kriva čelika za cevi API X65, /41/

The MFMC is modified by Wallin. By combining Eq. (29) with (31), he obtains:

$$K_0 = 31 + 77 \exp\left(0.019\left[T - T_{0,T_{stress}=0} - \frac{T_{stress}}{12\frac{\text{MPa}}{^\circ\text{C}}}\right]\right) \qquad (34)$$

K_0 represents the lower bound of the notch fracture toughness because it is determined with pre-cracked specimens. A similar MFMC is made for the notch fracture toughness /41/ of notched specimens like the Charpy and obtained from the fracture energy U_c:

$$J_{\rho,c} = \frac{\eta U_c}{Bb} \tag{35}$$

where B is the thickness and b the ligament size. Eta (η) is a parameter for the proportionality between the specific fracture energy per ligament area and the notch fracture toughness. It depends on the notch radius and relative notch depth a/W. Akkouri et al. /42/ tabulated the values of *eta* for different notch radii and relative notch depths. All data are fitted to the following equation:

$$J_{\rho,c} = A_{J,\rho} + B_{J,\rho} \tanh\left[\frac{(\Delta T^*)}{c_{K,\rho}}\right] \tag{36}$$

with
$$\Delta T^* = T - T_{t,T_{ef,c}=0} - 0.14 T_{ef,c} \tag{37}$$

ΔT^* represents the shift of the test temperature with the transition temperature in function of constraint $T_{ef,c}$. $T_{t,Tef,c=0}$ is the transition temperature corresponding to a constraint equal to zero and used as reference (197 K for API X65 pipe steel).

The definition of a general constraint-dependent master curve reference temperature $T_0(Y)$ results in the introduction of a material parameter T_0, which additionally depends on the actual loading situation. This implies a proper separation of material and loading parameters.

This problem was avoided in /40/, by the use of a master curve defined as an exponential function. One of the basic features of this type of function is that a shift in the direction of the argument coincides with a scaling of the function itself. A constraint-dependent scaling of the stress intensity factors according to:

$$K_J^{ref}(T,Y) = 30\ \text{MPa}\cdot\text{m}^{1/2} + \left(K_J(T) - 30\ \text{MPa}\cdot\text{m}^{1/2}\right)\times \\ \times \exp\left[0.019c(Y - Y^{ref})\right] \tag{38}$$

where Y_{ref} denotes the constraint parameter for a reference case. Through this procedure, a constraint indexing master curve reference temperature T_0^{CI} is established, defining a material curve that is independent of the actual loading situation. Values of Y_{ref} and T_0^{CI} for nuclear grade 22 NiMoCr 3-7 pressure vessel steel are given in Table 3.

T STRESS AND CRACK PATH

Cotterel /43/ has pointed out the role of T stress in crack curving. The T stress is a stress which acts parallel to the crack direction. Therefore, this stress combined with the opening stress induces a mixed mode of loading with a biaxiality ratio Θ:

$$\Theta = \frac{T\sqrt{\pi a}}{K_I} \tag{39}$$

The maximum stress along the $\sigma_{\theta\theta}$ distribution is not always null for $\theta = 0$ and angular deviation can occur only for positive values of T stress. When the T stress is negative, the maximum $\sigma_{\theta\theta}$ is always along the direction of propagation $\theta = 0$.

If T stress is positive, the crack curves according to the criterion of maximum tangential stress introduced by Erdogan and Sih, /44/. By applying this criterion, the opening stress is given by

$$\sigma_{\theta\theta} = \frac{K_I}{\sqrt{2\pi r}}\left[\frac{3}{4}\cos\frac{\theta}{2} + \frac{1}{4}\cos\frac{3\theta}{2}\right] + T\sin^2(\theta) \tag{40}$$

$$\frac{\sqrt{2\pi r}\cdot\sigma_{\theta\theta}}{K_I} = \left[\frac{3}{4}\cos\frac{\theta}{2} + \frac{1}{4}\cos\frac{3\theta}{2}\right] + \frac{T\sqrt{2\pi r}}{K_I}\sin^2(\theta) \tag{41}$$

The evolution of the ratio $\sqrt{2\pi r}\cdot\sigma_{\theta\theta}/K_I$ with the direction of propagation θ is plotted in Fig. 16 for positive or negative values of T. The maximum opening stress is indicated by a black spot for positive T stress. For negative T stress, this maximum occurs for negative values of opening stress and bifurcation cannot occur because the crack surfaces cannot overlap, /48/.

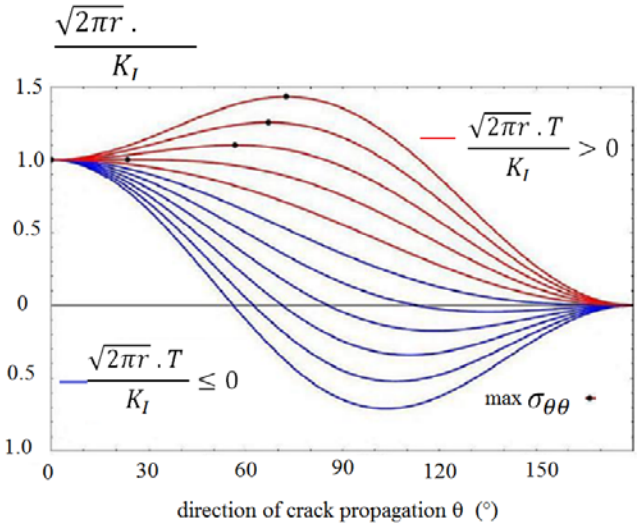

Figure 16. Evolution of the ratio $\sqrt{2\pi r}\cdot\sigma_{\theta\theta}/K_I$ with crack propagation direction θ in the presence of T stress, /45/.

Slika 16. Evolucija odnosa $\sqrt{2\pi r}\cdot\sigma_{\theta\theta}/K_I$ prema pravcu razvoja prsline θ u prisustvu T napona, /45/

The bifurcation direction θ^* is given when the first derivative of Eq.(41) is equal to zero.

$$\theta^* = \cos^{-1}\left[\frac{1 + \sqrt{1 + \frac{1024\pi}{9}X_{ef}\left(\frac{T_c}{K_{Ic}}\right)^2}}{\frac{512\pi}{9}X_{ef}\left(\frac{T_c}{K_{Ic}}\right)^2}\right] \tag{42}$$

and the second derivative must be negative. Chao et al. /22/ introduced the RKR criterion in this analysis. At fracture $K_I = K_c$, $T = T_c$ and $\sigma_{\theta\theta} = \sigma_c$ for $x = X_{ef}$. The bifurcation direction is θ^* and X_{ef} is the size of the fracture process volume or effective distance. The condition on the second derivative implies that for crack curving

$$\frac{T_c}{K_c} > \frac{3}{8}\frac{1}{\sqrt{2\pi X_{ef}}} \tag{43}$$

Figures 17 and 18 give an example of a DCB specimen with positive T stress and crack curving. The CT specimen also has a positive T stress and non-curving crack.

For negative T stress, after initiation, the crack propagates firstly in an instable manner and secondly after sev-

eral millimetres in a stable manner. During crack propagation in a stable manner, crack tip opening angle CTOA remains constant and its constant value is a characteristic of the fracture resistance of the material. It can be noted that during the stable crack propagation, both CTOA and T stress are constant (Fig. 19).

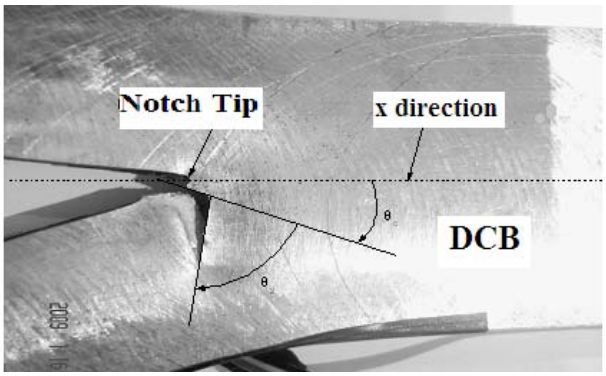

Figure 17. DCB with positive T-stress-induced crack curving $T/K = +7.9$; $X_{ef} = 0.53$ mm.
Slika 17. DCB epruveta sa pozitivnim skretanjem prsline, izazvanim T naponom, $T/K = +7{,}9$; $X_{ef} = 0{,}53$ mm

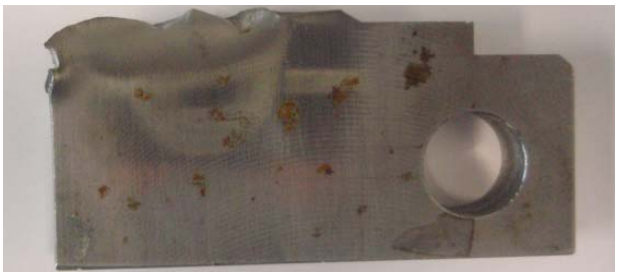

Figure 18. CT with positive T-stress-induced crack curving $T/K = +2.05$; $X_{ef} = 0.49$ mm.
Slika 18. CT epruveta sa pozitivnim skretanjem prsline, izazvanim T naponom, $T/K = +2{,}05$; $X_{ef} = 0{,}49$ mm

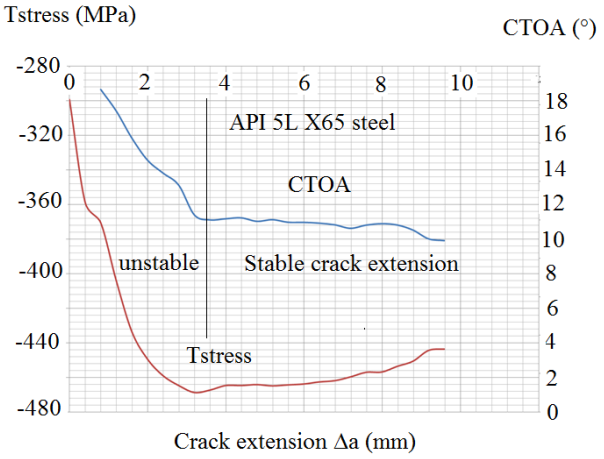

Figure 19. Evolution of CTOA and T stress during crack propagation. Steel API 5L X65.
Slika 19. Razvoj CTOA i T napona pri rastu prsline. Čelik API 5L X65

EFFECT OF THICKNESS ON FRACTURE TOUGHNESS AND OUT-OF-PLANE CONSTRAINT

It is well known now that fracture toughness (K_c or J_c) decreases when the thickness increases. The fracture toughness is maximal for plane stress conditions and trends asymptotically to a minimum called K_{Ic} or J_{Ic} if the plane strain conditions are satisfied. Therefore a description of fracture resistance cannot be done with a single parameter. Zhao and Guo /46/ proposed to describe the effect of thickness B on fracture toughness $K_c = f(B)$ by introducing 'a triaxial stress constraint' T_z. This parameter is defined as:

$$T_z = \frac{\sigma_{zz}}{\sigma_{yy} + \sigma_{xx}} \tag{44}$$

For a straight crack through the thickness, which is a typical case of 3D cracks, y is the direction normal to the crack plane $x0z$. In an isotropic linear elastic cracked body, T_z ranges from 0 to N, $T_z = 0$ for the plane stress state, and $T_z = N$ for the plane strain state, where N is the strain hardening exponent of the Ramberg-Osgood strain-stress relationship.

In order to take into account the thickness effect, it is necessary to have 3D descriptions of the singularity and angular distribution of stresses and strains as a function of the triaxial stress constraint T_z:

$$\begin{aligned} \sigma_{ij} &= \left[\frac{J}{\alpha\varepsilon_0\sigma_0 I(T_z,N)r}\right]^{1/N+1} \tilde{\sigma}_{ij}(\theta,T_z) \\ \varepsilon_{ij} &= \frac{3}{2}\alpha\left[\frac{J}{\alpha\varepsilon_0\sigma_0 I(T_z,N)r}\right]^{N/N+1} \tilde{\varepsilon}_{ij}(\theta,T_z) \end{aligned} \tag{45}$$

These forms are similar to that of an HRR solution, but J may be path dependent and I is a function of T_z and N. α is the coefficient of the Ramberg-Osgood law; σ_0 the reference stress, and ε_0 the strain associated to the reference stress. $\tilde{\sigma}_{ij}(\theta,T_z)$ and $\tilde{\varepsilon}_{ij}(\theta,T_z)$ are eigenvalues. I is a complex function of eigenvalues of stresses and displacements.

With this kind of stress distribution the T stress depends on relative thickness $z_B = z/B$ and is expressed as

$$T = \sigma_g \bar{T}(\nu, z_B) \tag{46}$$

where the function $\bar{T}$ presents a non-dimensional function and can be given as:

$$\bar{T}(\nu, z_B) = B_0 + \frac{B_1 \exp(z_B - B_2)}{B_3} \tag{47}$$

B_0, B_1, B_2, and B_3 are coefficients in function of the Poisson ratio ν.

For a pure mode I cracked plate, Zhao and Guo /46/ developed a 3D fracture criterion considering the out-of-plane stress constraint T_z. The thickness-dependent fracture toughness is predicted using the equivalent thickness concept. This means that the in-plane distribution of T_z at the point P is the same as that at the mid-plane of a plate with a thickness of B_{eq}:

$$B_{eq} = \left(1 - z_B^2\right) \tag{48}$$

The three-dimensional fracture toughness in the pure mode I, $K_{Iz,c}$, is a function of the fracture toughness associated with different thicknesses as:

$$K_{Iz,c} = K_c(B)\sqrt{f\left(\bar{T}_{zI}(B_{eq})\right)} \tag{49}$$

$$f\left(\bar{T}_{zI}(B_{eq})\right)=\frac{2}{3}(1+\nu)+\frac{4}{3}(1-2\nu)\left(\frac{1+\bar{T}_{zI}}{1-2\bar{T}_{zI}}\right)^2 \quad (50)$$

$$T_{zI}=\frac{1}{\bar{r}_p B_{eq}}\int_0^{\bar{r}_p}\int_0^{B_{eq}}\bar{T}_{zI}\,dz\,dr \quad (51)$$

where $\bar{r}_p$ is the mean radius of the crack-tip plastic zone along the thickness.

Zhao and Guo /46/ have tested this model on LY12-CZ aluminium alloy standard CT specimens. Figure 20 indicates that the fracture toughness of this alloy is strongly dependent on the thickness. After considering the equivalent thickness B_{eq} from Eq.(48), we can find that the three-dimensional fracture toughness in pure mode I, $K_{Iz,c}$, is almost a constant and is independent of the thickness.

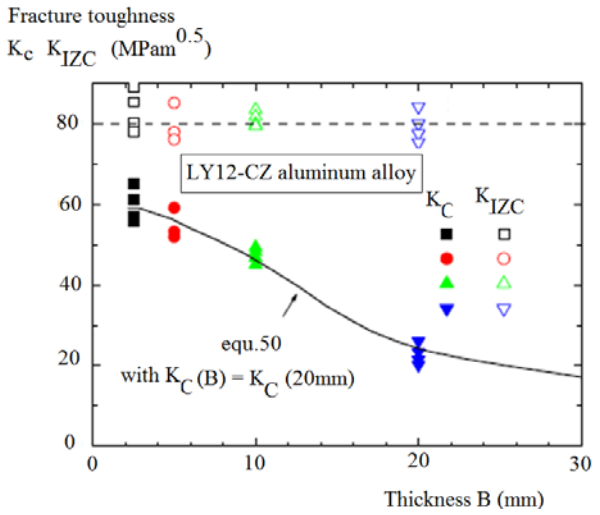

Figure 20. Determination of the 3-dimensional fracture toughness in pure mode I, $K_{Iz,c}$, on LY12-CZ aluminium alloy, /46/.
Slika 20. Određivanje trodimenzionalne žilavosti loma u uslovima opterećenja tipa I, $K_{Iz,c}$, kod legure aluminijuma LY12-CZ, /46/

CONCLUSION

Most of the problems of transferability in fracture toughness can be treated with the help of a constraint parameter or a characteristic length.

If a constraint parameter is required, the question arises - which of the different possibilities to choose (T, Q, β, L, A_2, A_P, φ, and so on).

The constraint parameters A_P and φ have been very recently introduced, in 2011 and 2014 respectively /32, 33/. No other papers have been published on these parameters which confirm their applicability. The parameter A_2 is similar to T ($T = 4A_2$). In the light of these considerations, our discussion will be focused on the following four parameters: T, Q, β, L.

T stress according to its definition is only used for elastic situations but is often extended to elastic plastic fracture.

Q is used only for elastic plastic fracture. We have seen that for pure brittle fracture, the Q parameter reduces to a relative difference of fracture toughness K_{Ic} (Eq.(15)).

L is used strictly for plastic collapse in order to calculate limit load.

Stress triaxiality β is used for any stress strain behaviour.

Determination of T stress needs only a single fracture test. This is an advantage compared with the Q parameter. A second advantage is that it can be determined numerically or experimentally. This is particularly interesting in the case of a complex part of a structure. The major difficulty with the T stress concept is that T stress is not constant along a ligament ahead of a defect. Therefore a conventional value is needed. It has been proposed to use the effective distance, /10/, or extrapolation of the T stress evolution to origin, /25/, but these two definitions are not always in agreement.

The point of the Q parameter is to obtain an idea of the relative shift of the opening stress distribution at defect tip. It suffers from the following problems:

i) its definition is purely conventional at a non-dimensional distance of ($\sigma_0 r/J = 2$) which rarely corresponds to the characteristic or the effective distance.

ii) Q is valid with a condition of homothety of the stress distribution given by Eq.(13). For low strength steels, this condition is not generally fulfilled.

Q determination needs two tests, the second as reference, which has to be performed according to small-scale yielding conditions. This is not easy to realise if the material does not have the required thickness.

The plastic constraint L represents the elevation of the net stress compared with the gross stress. It is difficult to define the net stress value which should be taken into account because the stress distribution is not constant over the ligament. Several definitions can be used: the maximum local stress, the effective stress or the average stress. A comparison of these definitions has been made by /7/. A definition based on a local failure criterion, the volumetric method, is certainly a more realistic one.

The stress triaxiality has the main advantage that it can be used for any kind of failure (brittle, elastic plastic or plastic collapse). Because the stress triaxiality varies along the ligament, a conventional definition of the prescribed value is also necessary (this value can be the value of the maximum or correspond to the effective distance). Its sensitivity to geometrical parameters /49/ such as the relative defect length reduces its interest as a reliable constraint parameter.

Eisele and others /36/ have suggested that fracture toughness is a decreasing function of constraints T and Q. In order to answer this question, Hohe and others /40/ tested four two-parameter approaches, the K–T stress-, J–Q-, J–A_2, and J–β-concepts. They found that all four approaches are able to characterise the local constraint situation of the different specimen geometry types considered. In a master curve analysis, they showed that the master curve reference temperature depends approximately linearly on the respective secondary fracture parameters of all four concepts. This result was confirmed for notch fracture toughness versus critical effective T stress, $T_{ef,c}$, /10, 41/. The linear relationship between the transition temperatures and the critical effective T stress has been confirmed by /38-41/.

With regard to the literature, the T stress is used most often. Its popularity is probably because its determination

needs only one test and is easy numerically. Compendia of T stress solutions and experimental and numerical methods are available /34/ and numerous results have been published.

The results demonstrate that tensile notched specimens show lower negative constraint than bending specimens and, as a result, higher notch fracture toughness. Moreover, the DCB specimen exhibits positive value of the $T_{ef,c}$-stress, as observed by Eisele and others /36/ and Kabiri /54/. Analysis of published T stress values /10, 50-54/ indicates that the T values associated with the different specimen types are not always in the same order (see Table 5).

These contradictory results can be explained by the fact that the stress distribution at defect tip is nearly homothetic if only one geometrical or loading mode is modified. If two or more parameters change at the same time, this condition is not fulfilled.

To overcome these difficulties, the trend is to use a three-parameter approach by adding the gradient or the third term of Williams's expansion A_3. This approach seems difficult to introduce in design codes and standards. The actual design method consists of comparing the computed hot stress with a single material characteristic. Modification of this approach is not readily accepted by standards and codes committees. A three-parameter approach needs additional computing and additional data and therefore additional costs.

This leads to the conclusion that a universal and unique constraint parameter of fracture toughness transferability is not available. The only solution is to choose a parameter depending on the problems after checking whether the conditions of validity are fulfilled.

Table 5. Order of the associated T value according to different published results.
Tabela 5. Redosled odgovarajuće vrednosti T prema raznim objavljenim rezultatima

Reference and material	specimens	Associated T value
/10/ X52	SENT (a/W = 0.5), CT (a/W = 0.1;0.3; 0.5), DCB (a/W = 0.5), TR (a/t = 0.4; 0.5; 0.6)	$T_{SENT} > T_{CT} > T_{RT} > T_{DCB}$
/51/ ASTM 719 Grade A steel	CT (a/W = 0.5), SENB (a/W = 0.5)	$T_{SENB} > T_{CT}$
/52/ ASI 1405-180	SENT (a/W = 0.5), SENB (a/W = 0.5), DENT (a/W = 0.5), CCT (a/W = 0.5), CT (a/W = 0.6)	$T_{DENT} > T_{CCT} > T_{SENT} > T_{SENB} \sim T_{CT}$
/53/ FYO HY 100 Alloy steel	SENT (a/W = 0.65), SENB (a/W = 0.61), DENT (a/W = 0.61),	$T_{SENT} > T_{SENB} > T_{DENT}$
/54/ PMMA	SENT (a/W = 0.3-0.6), CT (a/W = 0.3-0.7), DCB (a/W = 0.1-0.7)	$T_{CT} \sim T_{DCB} > T_{SENT}$

REFERENCES

1. Sinclair, G.B., Chambers, A.E., *Strength size effects and fracture mechanics: what does the physical evidence say?* Engineering Fracture Mechanics, Vol 26, N°2 : 279-310, (1987).
2. Morrisson, J.L.M., *The yield of mild steel with particular reference of the effect of size of specimen*, Proc. of the Inst. of Mech. Eng., Vol 142, 1 : 193-223, (1939).
3. Carpinteri, A., *Decrease of apparent tensile and bending strength with specimen size: Two different explanations based on fracture mechanics*, International Journal of Solids and Structures, Vol 25, N°4 : 407-429, (1989).
4. Carpinteri, A., *Scaling laws and renormalisation groups for strength and toughness of disordered materials*, Int. J. Solids Structures, 31, N°3 : 291-302, (1994).
5. Bazant, Z.P., *Scaling law of quasi brittle fracture asymptotic analysis*, Int. J of Fracture, Vol 83 : 19-40, (1997).
6. Chechulin, B.B., *Influence of specimen size on the characteristic mechanical value of plastic fracture*, (in Russian), Zhur. Tekh. Fiz., Vol 24 : 1093-1100, (1954).
7. Mouwakeh, M., Pluvinage, G., Masri, S., *Failure of water pipes containing surface cracks using limit analysis notions*, Res. J of Aleppo Univ. Engineering Science Series, Vol 63, (2011).
8. Henry, B.S., Luxmore, A.R., *The stress triaxiality constraint and the Q-value as a ductile fracture parameter*, Engng. Fracture Mechanics, Vol 57 : 375-390, (1997).
9. Ruggieri, C., Gao, X., Dodds, R.H., *Transferability of elastic-plastic fracture toughness using the Weibull stress approach: Significance of parameter calibration*, Engng. Fracture Mechanics, Vol 67 : 101-117, (2000).
10. Hadj Meliani, M., Matvienko, Y.G., Pluvinage, G., *Two-parameter fracture criterion ($K_{\rho,\chi}$-$T_{ef,c}$) based on notch fracture mechanics*, Int. J of Fracture, Vol 167: 173-182, (2011).
11. Nikishkov, G.P., *An algorithm and computer program for the three-term asymptotic expansion of elastic-plastic crack tip stress and displacement field*, Engng Frac Mech; Vol 50 : 65-83, (1995).
12. Aifantis, E.C., *The physics of plastic deformation*, Int. J of Plasticity, Vol.3 : 212-247, (1987).
13. Brandt, A., *Calcul des pièces à la fatigue par la méthode du gradient*, Editor CETIM, (In French), (1980).
14. Adib-Ramezani, H., Jeong, J., *Advanced volumetric method for fatigue life prediction using stress gradient effects at notch roots*, Comput. Materials Science, Vol 39 : 649-663, (2007).
15. Matic, P., Kirby, G.C., Jolles, M.I., *The relation of tensile specimen size and geometry effects to constitutive parameters for ductile materials*, Proc. Roy. Soc., London, A, Vol 417 : 309-333, (1988).
16. Williams, M.L., *On the stress distribution at the base of stationary crack*, ASME J Appl Mech, Vol 24:109-114, (1957).
17. Larsson, S.G., Carlsson, A.J., *Influence of non-singular stress terms and specimen geometry on small-scale yielding at crack tips in elastic-plastic materials*, J Mech Phys Solids 1 Vol (21), : 263-77, (1973).
18. Hutchinson, J.W., *Singular Behavior at the End of a Tensile Crack in a Hardening Material*, J of Mechanics and Physics of Solids, Vol.16 : 13-31, (1968).
19. O'Dowd, N.P., Shih, C.F., *Family of Crack-Tip Fields Characterized by a Triaxiality Parameter: Part I - Structure of Fields*, J Mech. and Physics of Solids, Vol. 39 : 989-1015, (1991).
20. O'Dowd, N.P., Shih, C.F., *Family of Crack-Tip Fields Characterized by a Triaxiality Parameter: Part II - Fracture Applications*, J Mech. and Physics of Solids, Vol.40 : 939-963, (1992).
21. Yang, B., Ravichandar, K., *Evaluation of T stress by stress difference method*, Engng Fract Mech., Vol.64 :589-605, (2001).
22. Chao, Y.J., Liu, S., Broviak, B.J., *Brittle fracture: variation of fracture toughness with constraint and crack curving under mode I conditions*, Exp Mech ; Vol 41 :232-41, (2001).
23. Ayatollahi, M.R., Pavier, M.J., Smith, D.J., Mode I cracks subjected to large T stress, Int J Fract; Vol 117:159-74, (2002).
24. Hadj Meliani, M., Azari, Z., Pluvinage, G., Matvienko, Yu.G., *The Effective T-stress Estimation and Crack Paths Emanating from U-notches*, Engng Fracture Mechanics, Vol 77, Issue 11, July : 1682-1692, (2010).

25. Maleski, M.J., Kirugulige, M.S., Tippur, H.V., *A Method for Measuring Mode I Crack Tip Constraint Under Static and Dynamic Loading Conditions*, Soc. for Experimental Mech., Vol. 44, No.5, October, (2004).
26. Dodds, R., Ruggieri, C., Koppenhefer, K., *3D Constraint effects on models for transferrability of cleavage fracture toughness*, ASTM 1321: 179-197, (1997).
27. Rice, J.R., Tracey, D.M., *On the ductile enlargement of voids in triaxial stress fields*, J Mech. and Physics of Solids, Vol 26 : 163-186, (1969).
28. Kaechele, L.E., Tetelman, A.S., *A statistical investigation of microcrack formation*, Acta Metall., Vol.17 : 463-475, (1969).
29. Akourri, O., Elayachi, I., Pluvinage, G., *Stress Triaxiality as Fracture Toughness Transferability Parameter for Notched Specimens International*, Review of Mech Engng (I.RE.M.E.), Vol.1, N°6, November, (2007).
30. Chao, Y.J., Zhang, X., *Constraint effect in brittle fracture*, 27th National Symposium on Fatigue and Fracture, ASTM STP 1296. R.S. Piascik, J.C. Newman, Jr., and D.E. Dowling, Eds. ASTM Philadelphia : 41-60, (1997).
31. Chao, Y.J., Reuter, W.G., *Fracture of surface cracks under bending loads*, In: Underwood JH, MacDonald B, Mitchell M (eds), Fatigue and Fracture Mechanics, Vol.28, ASTM STP 1321, American Society for Testing and Materials, Philadelphia : 214-242, (1997).
32. Mostafavi, M., Smith, D.J., Pavier, M.J., *A micromechanical fracture criterion accounting for in-plane and out-of-plane constraint*, Comput Mater Sci ; Vol.50 : 2759-70, (2011).
33. Yang, J., Wang, G.Z., Xuan, F.Z., Tu, S.T., *Unified correlation of in-plane and out-of-plane constraint with fracture resistance of a dissimilar metal welded joint*, Engng Fracture Mech, Vol 115 : 296-307, (2014).
34. Sherry, A.H., France, C.C., Goldthorpe, M.R., *Compendium of T-stress solution for two and three dimensional cracked geometries*, Fatigue and Frac of Engng Mater and Struct, Vol.18 : 141-155, (1995).
35. Wang, E., Zhou, W., Shen, G., *Three-dimensional finite element analysis of crack-tip fields of clamped single-edge tension specimens – Part II: Crack-tip constraints for any pressure values and pipe diameter*, Engng Fract Mech, Vol.116 :144-157, (2014).
36. Eisele, U., Roos, E., *Evaluation of different fracture-mechanical J-integral initiation values with regard to their usability in the safety assessment of components*, Nuclear Engng and Design, Vo1.130 : 237-247, (1990).
37. Dlouhy, I., Holzmann, M., Chlup, Z., *Fracture resistance of cast ferritic C-Mn steel for container of spent nuclear fuel*, in: Transferability of Fracture Mechanical Characteristics, Ed. Dlouhy, NATO Sciences Series : 47-64, (2001).
38. Wallin, K., *Quantifying T-stress controlled constraint by the master curve transition temperature T_0*, Engng Frac Mech, Vol 68 : 303-28, (2001).
39. Wallin, K., *Structural integrity assessment aspects of the Master Curve methodology*, Engng Fract Mech, Vol.77: 285-292, (2010).
40. Hohe, J., Hebel, I., Friedmann, V., Siegele, D., *Probabilistic failure assessment of ferritic steels using the master curve approach including constraint effects*, Engng Fract Mech, Vol 74 : 1274-1292, (2007).
41. Coseru, A., Capelle, J., Pluvinage, G., *On the use of Charpy transition temperature as reference temperature for the choice of a pipe steel*, Engng Failure Analysis, Vol 37, February : 110-119, (2014).
42. Akourri, O., Louah, M., Kifani, A., Gilgert, J., Pluvinage, G., *The effect of notch radius on fracture toughness J_{Ic}*, Engng Frac Mech, Vol 65 : 491-505, (2000).
43. Cotterell, B., *Slightly curved or kinked cracks*, Int J Fracture, Vol.16, No.2, April, 155-169, (1980).
44. Erdogan, F., Sih, G.C., *On the crack extension in plates under loading and transverse shear*, Trans of the ASME. J Basic Engng, Vol 85 : 519-527, (1963).
45. Capelle, J., Ben Amara, M., Pluvinage, G., Azari, Z., (2014) *Role of constraint on the shift of ductile-brittle transition temperature of subsize Charpy specimens*, Fatigue Fract. Eng. Mater. Struct. 37, DOI: 10.1111/ffe.12212.
46. Zhao, J., Guo, W., *Three-parameter K-T-T_z characterization of the crack-tip fields*, in: Compact-tension-shear specimens, Engng Fract Mech, Vol 92 : 72-88, (2012).
47. Malmberg, Minutes of the task 5 group meeting, Joint Research Centre, EU project FI4S-CT96-0024, (1998).
48. Yao, W., *Stress intensity approach for predicting fatigue life*, Int J of Fatigue, Vol.15 : 243-251, (1993).
49. Akourri, O., Elayachi, I., Pluvinage, G., *Stress Triaxiality as Fracture Toughness Transferability Parameter for Notched Specimens International*, Review of Mechanical Engineering (I.RE.M.E.), Vol.1, N°6, November, (2007).
50. Hancock, J.W., Reuter, W.G., Parks, D.M., *Constraint and toughness parameterised by T*, in: EM Hackett, KH Schwalbe, RH Dodds, Eds, Constraint effect in Fracture, ASTM STP 1171, ASTM, Philadelphia, PA : 21-40, (1993).
51. Wu, S., Mai, Y.W., Cotterell, B., *Prediction of initiation of ductile fracture*, J Mech Phys Solids, Vol 43 :793-810, (1995).
52. Joyce, J.A., Hackett, E.M., Roe, C., *Comparison of J_{Ic} and J-R curves for short cracks and tensilely loaded specimen geometries of high strength structural steel*, NUREG CR-5879 US Nuclear Regulatory Commission , (1992).
53. Liu, S., Chao, Y.J., *Variation of fracture toughness with constraint*, Int J Fracture, Vol.124 : 113-117, (2003).
54. Kabiri, M.R., *Fissuration des aciers à haute température, effet de la géométrie sur la transférabilité des lois de propagation*, Thèse Ecole des Mines de Paris, (2003).